Scientific
Research

# ZnO Heteroepitaxy on Sapphire Using a Novel Buffer Layer of Titanium Oxide: Optoelectronic Behavior

## Satoshi Yamauchi[1*], Yoh Imai[2]

[1]Department of Biomolecular Functional Engineering, Ibaraki University, Hitachi, Japan
[2]Department of Electric and Electronic Engineering, Ibaraki University, Hitachi, Japan
Email: *ysatoshi@mx.ibaraki.ac.jp

## ABSTRACT

Optoelectronic property of ZnO epitaxial layer grown by plasma-assisted epitaxy at temperature as low as 340°C using $Ti_2O_3$ buffer layer on a-sapphire were studied by low temperature photoluminescence at 10 K comparing to the layers on c-sapphire and a-sapphire without the buffer layer. The near band-edge emission consisting of free-exciton emissions and neutral-donor bound exciton emissions was significantly dependent on the buffer thickness and dominated by the free-exciton emissions in the layer grown on the very thin buffer layer about 0.8 nm, whereas the intense emissions by neutral-donor bound excitons were observed in the ZnO layer on c-sapphire. The structural behavior indicated the donor was originated from the three-dimensional growth of ZnO layer and details of the optoelectronic feature suggested the residual donors were Al and interstitial-Zn.

**Keywords:** ZnO; $Ti_2O_3$; Plasma-Assisted Epitaxy; Photoluminescence; Free-Exciton; Bound-Exciton

## 1. Introduction

ZnO is candidate for highly efficient blue or ultraviolet light-emitting devices using the wide direct band gap of 3.37 eV and the large exciton binding energy of 60 meV at room temperature. For such device applications, advanced processes are required for the high-quality growth and highly efficient impurity doping. To date, MBE using oxygen-plasma cell [1], MOMBE using $H_2O$ vapor [2], PLD [3] etc. have been attractively studied to improve the structural and optoelectronic properties. At the first stage for ZnO growth, reduction of oxygen deficiency which generates strong green-emission due to oxygen vacancies in ZnO had been required to improve the optoelectronic property. For the purpose, plasma-assisted epitaxy (PAE) using oxygen gas plasma was also an useful process as demonstrated for undoped-ZnO growth at the temperature as low as 400°C on c-sapphire [4,5], in which the green-emission was sufficiently decreased comparing to the band-edge emissions. However, the near band-edge emissions were dominated by neutral donor bound emissions as same as the other processes, which indicated unexpected shallow donors were included with relatively high-density in the layer. It is important to prevent the donors during ZnO growth, especially for p-type ZnO growth. Therefore, the origin and the removal process have been studied at the second stage, in addition to the effective acceptor doping into the layer [6,7]. As well recognized, low-temperature photoluminescence (PL) is so useful for evaluation of the impurities. In the case of ZnO, the bound exciton emissions concerned with shallow donor impurities such as Ga, Al, In and H have been established with the free-exciton emissions [8]. In addition to such impurity donors, interstitial-Zn should also be taken into account for the shallow donor defect in ZnO as suggested by electron paramagnetic resonance [9]. In the growth process, the defect-donor can be easily introduced during three-dimensional growth of ZnO by high-sticking coefficient of Zn-adatom at steps or kinks on the growth surface. Further, the unfavorable feature is probably enhanced in non-equilibrium growth at low temperatures required for highly efficient doping. Therefore, suitable two-dimensional ZnO growth at low temperatures with reducing impurity-donors and the intrinsic donor-defects is required for the optoelectronic device applications. For the purpose, we previously demonstrated drastic improvement of ZnO growth by $Ti_2O_3$ buffer layer on a-sapphire [10], where two-dimensional epitaxial growth of ZnO layer was successfully achieved without the rotational domain.

In this paper, optoelectronic property of PAE-ZnO layer grown on the $Ti_2O_3$ buffer layer is examined by low-temperature photoluminescence and shows significant reduction of the residual donor. In addition, details of the near band-edge emissions suggest the donor species.

## 2. Experimental

### 2.1. Layer Growth

Titanium oxide layer was grown by LPCVD using titanium tetra-iso-propoxide (TTIP: $Ti-(OC_3H_7)_4$) and oxygen gas. Details of the apparatus and the condition was shown elsewhere [10]. In the case of buffer layer growth for ZnO layer, the thickness was controlled by the growth period estimated from the growth rate.

ZnO layer was grown at 340˚C or 400˚C in 3 mtorr by plasma-assisted epitaxy (PAE) using oxygen gas plasma generated by 10 W radio-frequency (rf) power at 13.56 MHz through a capacitively coupled rf-electrode. Details of the PAE-apparatus and the growth process were described elsewhere [4,10]. ZnO growth rate was different by change of the growth mode on c-, a- and the buffer layer as shown elsewhere [10], but effective Zn/O supply ratio during the growth was kept at 1.0 by control of Zn-flux determined by dependence of the growth rate on the Zn-flux.

Single crystalline a- and c-sapphire with mirror surface and 300 μm-thick were used as substrates after cleaning by organic-solvents and hot $H_2SO_4 + H_2O_2$. In the case of etching, the substrates were treated in a hot $3H_2SO_4 + H_3PO_4$ solution at 130˚C for 15 min.

### 2.2. Evaluation

Thickness of ZnO layers and $Ti_2O_3$ layers were checked by a contact-type surface profiler (Veeco, DEKTAK150). Surface morphology of the ZnO films was observed by Nomarski differential interference microscope (OLYMPUS, BX60). Optoelectronic property was examined by photoluminescence (PL) at 10 K using a cryogenic system (Janis Research, CCS-150). UV-light around 313 nm radiated from a deep UV-lamp (USHIO, UXM-501MA) was selected by a band-pass filter and irradiated on the ZnO layer through a sapphire window equipped on the cryostat chamber with the light power density about 2 $mW/cm^2$. The luminescent light modified to 20 Hz-AC by an optical chopper was introduced into a monocrometor (JASCO, SS-50), then detected and amplified by a photomultiplier (Hamamatsu R374) driven by 1 kV. The current signal was amplified and converted to voltage signal by an amplifier (FEMTO, DLPCA-200), and then the noise components was removed in lock-in-amplifier (NF, LI5640) synchronous to the frequency by the chopper. Then, the signal was recorded in a PC after A/D

conversion. The relative sensitivity of the system for photon energy was corrected by black-body radiation spectrum from a standard lamp.

## 3. Results and Discussions

### 3.1. ZnO Layer on C-Sapphire

Growth rate of ZnO layers at 400˚C (closed circles) and 340˚C (open circles) on c-sapphire for various Zn-flux in oxygen plasma excited by 10 W rf-power are shown in **Figure 1**. The growth rates same at both temperatures were increased with the Zn-flux then saturated by the flux above 80 μmol/min. The results indicated the effective supply flux rate of Zn/O could be determined at both temperatures since the growth rate was limited by smaller flux of Zn or O. **Figure 2** shows typical near band-edge PL spectrum of PAE-ZnO layer with the thickness of 1.0 m grown at 400˚C on c- sapphire by the Zn/O supply ratio of 1.0 (Zn-flux: 80 μmol/min). The inset shows surface morphology of the layer observed by Nomarski microscope. The layer consisting of three-dimensionally grown columnar grains was preferentially oriented along c-axis but including 30˚-rotational domains. In the PL spectrum, prominent emission peak at 3.3623 eV originated from neutral donor-bound exciton emission (DBE) was observed with a weak DBE emission peak 3.3666 eV and free-exciton emissions of A-$E_x$ and B-$E_x$ at 3.3774 eV and around 3.385 eV respectively [8]. FWHM of the DBE emission of the layer grown by the supply ratio around 1.0 was below 2 meV and the intensity was 4-orders magnitude larger than the green-emission due to deep-level. It is noted that the PL-spectrum was obviously degraded in the ZnO layer grown at temperatures lower than 400˚C and the sharp near band-edge emissions could not be observed.
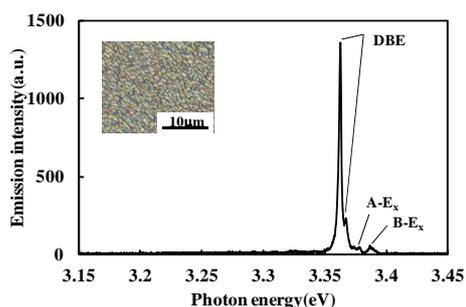
### 3.2. ZnO Layer on $Ti_2O_3$ Buffer Layer

#### 3.2.1. PL Spectrum on A-Sapphire and Buffer Layer
**Figure 3** shows near band-edge spectra of PAE-ZnO layers grown on (a) a-sapphire and (b) $Ti_2O_3$ buffer layer grown at 320˚C with the thickness of 0.8 nm, where the ZnO layers were grown at 340˚C in oxygen plasma excited by 10 W rf-power. It is noted here the near band-edge emissions could be observed in ZnO layers grown at the temperature around 340˚C but obviously degraded by the high temperature growth around 400˚C. The insets show the surface morphologies observed by Nomarski microscope. The layer was epitaxially grown on the buffer layer with the epitaxial relationship of [1-100] ZnO//[1-100] $Ti_2O_3$, whereas the layer was polycrystallized on a-sapphire. The hexagonal pyramid-like grains with the facets according to the epitaxial relationship as shown in the inset of (b) were observed in ZnO
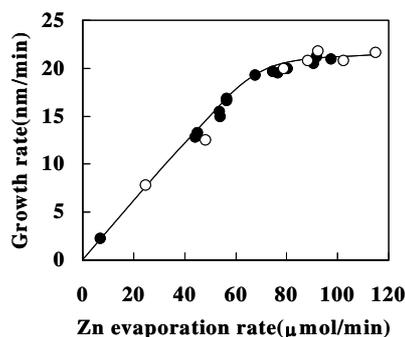
**Figure 1. Dependence of ZnO growth rate on Zn-flux, where the ZnO layers were grown on c-sapphire at 400˚C (solid circle) and 340˚C (open circle) in oxygen plasma excited by 10W rf-power.**



**Figure 2. Photoluminescence spectrum of PAE-ZnO layer on c-sapphire.**
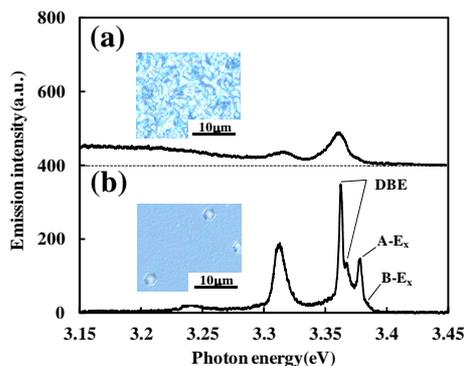


**Figure 3. Photoluminescence spectra of PAE-ZnO layer on (a) c-sapphire and (b) 0.8 nm-thick Ti$_2$O$_3$/a-sapphire.**

layer on the buffer layer, which indicated the two-dimensional growth was enhanced on the buffer layer as described elsewhere [10]. In the near band-edge PL-feature, strong and sharp exciton emissions could be observed from ZnO layer on the buffer layer, in contrast to board and weak emissions from poly-crystallized ZnO layer directly grown on a-sapphire. The spectrum of **Figure 3(b)** was dominated by DBE emissions with the same peak energies in **Figure 2** (grown on c-sapphire), however, free-exciton emissions of A-E$_x$ and B-E$_x$ were clearly observed with decreasing the DBE intensities. The results indicate that although the ZnO layer was

grown at low temperature comparing to the growth on c-sapphire, the crystallinity was improved on the buffer layer. In addition, the residual shallow donor could also be reduced in the ZnO on the buffer layer.

### 3.2.2. Dependence on the Buffer-Layer Growth Condition

The PL feature was significantly dependent on the growth condition and the thickness of buffer layer. **Figure 4** shows variation of the intensity ratio of A-E$_x$ to DBE emission peak at 3.3623 eV on the thickness of buffer layer grown at 320˚C and 340˚C (closed circles) with the intensity of A-E$_x$ emission (open circles). Crystal quality should not be discussed only by the intensity ratio because PL-spectrum is also influenced by non-radiative defects, but it can be considered the free-exciton emission intensity suggests the quality. In the case of 340˚C growth of the buffer layer, A-E$_x$ emission in ZnO layer on the 1.8 nm-thick buffer layer was most intense, but optimized the thickness of buffer layer for the intensity ratio of A-E$_x$/DBE was around 2.8 nm since not only the intense A-E$_x$ but also strong donor bound exciton emission were observed from ZnO layer on the 1.8 nm-thick buffer layer. The result indicated non-radiative defects were significantly reduced in ZnO layer on the buffer layer with the thickness around 1.8 nm comparing to the ZnO layers on c-sapphire but the donor could not be reduced in the ZnO layer. In contrast, when the buffer layer was grown at 320˚C, the PL-property was more sensitive to the buffer layer thickness, but the thickness could be optimized at 0.8 nm for both of A-E$_x$ intensity and the intensity ratio. The layer grown on the optimized buffer layer grown at 320˚C showed smooth surface partially including hexagonal pyramid-like grains as shown in **Figure 3(b)**, where the number of pyramid-like grain was most reduced in the ZnO layer on the optimized buffer layer [10]. It was found that the pyramid-like grains were originated from surface roughness and dislocations on a-sapphire and could be prevented by chemical etching of the substrate using a hot $3H_2SO_4 + H_3PO_4$ solution. It is noted that density of the pyramid-like grains were decreased but columnar grains without the fine facets observed in the pyramid-like grains were increased with the buffer thickness above 2 and 4 nm for the growth temperature of 320˚C and 340˚C, respectively.

### 3.2.3. PL Spectrum of ZnO Layer on Optimized Buffer-Layer

**Figure 5** shows near band-edge PL-spectrum of ZnO layer on 0.8 nm-thick buffer layer grown at 320˚C on chemically etched a-sapphire. As shown in the inset, hexagonal pyramid-like grains were almost disappeared in the ZnO layer. In comparison to **Figure 3(b)**, donor
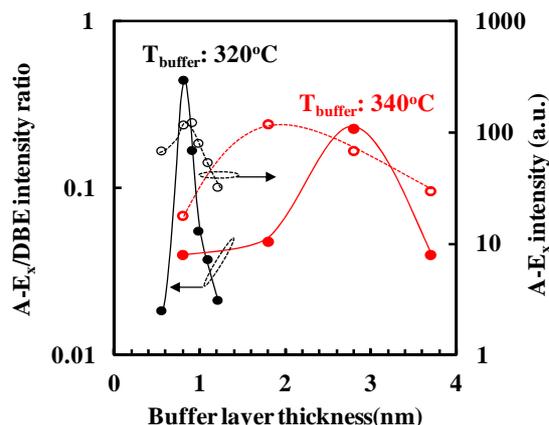
**Figure 4. Dependence of A-Ex/DBE intensity ratio (closed circles) and A-E$_x$ intensity (open circles) on the thickness of Ti$_2$O$_3$ buffer layer grown at 320$^\circ$C (black) and 340$^\circ$C (red).**
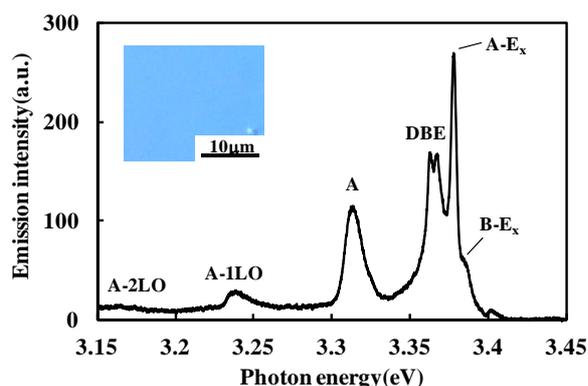


**Figure 5. Photoluminescence spectra of PAE-ZnO layer on 0.8 nm-thick Ti$_2$O$_3$/a-sapphire, where the a-sapphire was chemically etched by a hot 3H$_2$SO$_4$ + H$_3$PO$_4$ solution at 130$^\circ$C for 15 min before the Ti$_2$O$_3$ growth.**

bound exciton emissions were drastically decreased and dominated by intense and sharp A-E$_x$ with the FWHM below 5 meV. The fine feature clearly indicated residual donor was successfully reduced during the ZnO growth and the three-dimensional growth increased the donor density.

Broad-line around 3.313 eV denoted "A", which was shifted between 3.313 - 3.315 eV by the ZnO growth condition, with the photon-replicas (LO-phonon energy: 73 meV) was also observed in the ZnO layers. The emission was seemed to be similar to emission discussed as A-line [11], which was concluded as surface defects-related emission. The thermal activation energy of the broad-line obtained by Arrhenius-relationship on the intensity was about 60 meV, which indicated the emission was not due to electron recombination in deep-level but originated from recombination of exciton bound to defects. Further, the emission was not observed from the ZnO layer on c-sapphire as shown in **Figure 2**, which indicated the emission was not derived from the grain

boundaries. The origin of defect bounding exaction is not identified yet, but may be related to surface structural defects [11,12].

### 3.2.4. Residual Donor

It has been well recognized a lot of sharp donor bound exciton emission lines in the narrow energy range from 3.348 to 3.373 eV [8], in which the lines are due to neutral or ionized donor defect pair [8,13]. **Figure 6** shows PL spectra in log-scale of ZnO layers on (a) buffer layer and (b) c-sapphire. The bound exciton emission peak at 3.3623 eV could be assigned to be due to neutral donor bound exciton with the localization energy of 15.1 meV from the A-E$_x$ with peak at 3.3774 eV. Impurities corresponding to neutral donor bound exciton emissions have been identified in bulk-ZnO for IIIB-elements such as Al, Ga and In [8]. Although peak energy of the neutral donor bound exciton emission was different from the impurity related bound exciton emission as previously reported, the localization energy of 15.1 meV was coincident to the binding-energy of Al. The exciton line bound to hydrogen at 3.363 eV [14] was in agreement to the bound exciton in PAE-ZnO layer, but the impurity was rule out because the emission peak at 3.3623 eV was not decreased by annealing at 600$^\circ$C for 30 min whereas the emission bound to hydrogen-donor was drastically reduced by the annealing [14]. It is considered that the impurity can be identified by the localization energy from free-exciton emission because the free-exciton line is shifted by bi-axial stress [15]. The A-E$_x$ emission of PAE-ZnO was shifted toward higher energy side than that with peak 3.3759 eV (transversal free A-exciton state) dominated in A-exciton emissions bulk-ZnO [8]. As a result, it could be suggested that a residual donor in the PAE-ZnO layer was Al. Meyer, *et al*. showed Haynes'
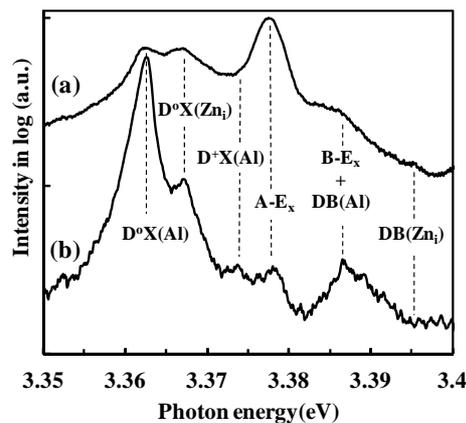


**Figure 6. Photoluminescence spectra in excitonic emission region of PAE-ZnO layers on (a) 0.8 nm-thick Ti$_2$O$_3$/a-sapphire and (b) c-sapphire, where the intensity was shown in log scale and the ground-line of (a) was shifted in vertical.**

rule in ZnO as $E_{loc} = 0.37E_D - 4.2$ meV for neutral donor bound exiton and $E_{loc} = 0.50E_D - 23$ meV for ionized donor bound exciton, where $E_{loc}$ and $E_D$ are activation energy of donor and localization energy of the bound excitons from free A-exciton, respectively [16]. According to the localization energy of 15.1 meV for the neutral donor bound exciton ($D^oX(Al)$), binding energy of the donor was obtained as 52.2 meV. In addition, localization energy the ionized donor bound exciton ($D^+X(Al)$) was expected to be at 3.1 meV by the above relationship. The exciton line could be observed as the weak emission around 3.374 eV on the low-energy side shoulder of the A-$E_x$ in (a) and at 3.3736 eV in (b). Further, the donor to valence-band (DB(Al)) emission was expected to be observed at 3.3852 eV, in which the band-gap was obtained by the A-$E_x$ line and the binding energy of 60 meV. It was difficult to identify the emission in PL spectrum because the emission line was overlapped on the B-$E_x$ emission, however, the intensity around 3.385 eV in the spectrum with intense $D^oX(Al)$ emission was larger than that of A-$E_x$ emission as shown in **Figure 6**(b).

On the other, the donor concerned to the emission line at 3.3666 eV with the localization energy of 10.8 meV could not be identified by the IIIB-impurities. Previously, Shibata, *et al.* indicated the emission at 3.366 eV is neutral donor bound exciton emission due to interstitial-Zn [17], where the localization energy was obtained as 11 meV because free-exciton emission was observed at 3.377 eV. The localization energy was in good agreement to that of the emission at 3.3666 eV in PAE-ZnO. The spectral feature broader than the $D^oX(Al)$ also suggested the emission at 3.3666 eV was due to exciton emission bound to interstitial-Zn complex ($D^oX(Zn_i)$). Binding energy of the donor was obtained to 40.5 meV and exciton will not be bound to the ionized donor with such shallow level ($E_D < 47$ meV) as recognized by the previous relationship [16]. In contrast, it is considered that the weak emission peak at 3.3955 eV in **Figure 6** (a) was the donor to valence-band emission (DB($Zn_i$)), in which the donor binding energy was obtained as 41.9 meV. It is noted that the emission of (DB($Zn_i$)) was not observed from ZnO layer including Al with relatively high density as shown in **Figure 6** (b).

Both of the $D^oX(Al)$ and $D^oX(Zn_i)$ were drastically reduced in the ZnO layer grown at 340˚C on the buffer layer comparing to that on c-sapphire grown at 400˚C. The Al was probably diffused from sapphire substrate because the $D^oX(Al)$ was drastically reduced in the ZnO layer grown at 340˚C on the buffer layer comparing to the layer on c-sapphire grown at 400˚C although Al on the growth surface was expected to be with higher sticking coefficient at lower temperature. Therefore, two possible effects can be considered for reduction of the donor in ZnO on the buffer layer. The one is decrease of

the growth temperature, which brings decrease of the diffusion coefficient. As expected increasing diffusion coefficient in grain boundaries, the other is concerned to structural behavior of ZnO layer, which can be expected by variation of A-$E_x$/$D^oX(Al)$ intensity ratio for the buffer layer thickness as shown in comparison to the growth behavior. That is, it is considered that the Al diffusion was suppressed in ZnO layer on the optimum buffer layer by significantly decreased grain boundaries. In contrast, interstitial-Zn is promised to be introduced on the surface during ZnO growth. Also in this case, it is expected that interstitial-Zn is easily introduced into the layer at low temperature, however, the $D^oX(Zn_i)$ was decreased by the buffer layer even at low temperature of 340˚C comparing to 400˚C for the growth on c-sapphire, which suggest that the surface structure is more important to prevent interstitial-Zn than the growth temperature. Further, the intensity ratio of A-$E_x$/$D^oX(Zn_i)$ of ZnO layer was drastically decreased on the buffer layer grown at 320˚C with thickness above 1.2 nm, where the three-dimensional ZnO growth was drastically enhanced and a lot of columnar-grains without facets were observed, however, the increased ratio of ZnO layer including pyramid-like grains on the buffer layer with optimized thickness as shown in **Figure 3(b)** was similar to that of the layer successfully removed the grains by sapphire-etching as shown in **Figure 4**. The results indicate interstitial-Zn is increased on the three-dimensional growth surface but prevented on hexagonal pyramid surface.

## 4. Conclusion

Optoelectronic property of PAE-ZnO layers grown on c-sapphire, a-sapphire and $Ti_2O_3$ buffer layer was examined by PL at low temperature of 10K. Neutral donor bound exciton emissions were dominated in the near band-edge region of ZnO layer on c-sapphire. In contrast, although the PL feature was significantly dependent on the buffer layer thickness and the growth condition, successful reduction of donor bound exciton emissions by the optimized buffer layer were resulted in the spectrum dominated by free-exciton emissions. The residual donors in the ZnO layer could be identified as Al and interstitial-Zn by the localization energy of the neutral bound exciton emissions from free-exciton emission. The obvious decrease of grain boundaries in ZnO layer was so effective to the Al-reduction in addition to low temperature ZnO layer was nominally decreased by the low temperature growth of 340˚C on the optimized buffer layer.

## REFERENCES

[1] M. A. L. Johnson, S. Fujita, W. H. Rowland, Jr., W. C. Hughes, J. W. Cook, Jr. and J. F. Schetzina, "MBE Growth and Properties of ZnO on Sapphire and SiC Sub-

      

strates," *Journal of Electronic Materials*, Vol. 25, No. 5, 1996, pp. 855-862. doi:10.1007/BF02666649

[2] A. B. M. A. Ashrafi, I. Suemune, H. Kumano and S. Tanaka, "Nitrogen-Doped p-Type ZnO Layers Prepared with $H_2O$ Vapor-Assisted Metalorganic Molecular-Beam Epitaxy," *Japanese Journal of Applied Physics*, Vol. 41, 2002, pp. L1281-L1284. doi:10.1143/JJAP.41.L1281

[3] R. D. Vispute, V. Talyansky, Z. Trajanovic, S. Choopun, M. Downes, R. P. Sharma, T. Venkatesan, M. C. Woods, R. T. Lareau and K. A. Jones, "High Quality Crystalline ZnO Buffer Layers on Sapphire (001) by Pulsed Laser Deposition for III-V Nitrides," *Applied Physics Letters*, Vol. 70, No. 20, 1997, pp. 2735-2737. doi:10.1063/1.119006

[4] S. Yamauchi, H. Handa, A. Nagayama and T. Hariu, "Low Temperature Epitaxial Growth of ZnO Layer by Plasma-Assisted Epitaxy," *Thin Solid Films*, Vol. 345, No. 1, 1999, pp. 12-17. doi:10.1016/S0040-6090(99)00096-6

[5] S. Yamauchi, T. Ashiga, A. Nagayama and T. Hariu, "Plasma-Assisted Epitaxial Growth of ZnO Layer on Sapphire," *Journal of Crystal Growth*, Vol. 214-215, 2000, pp. 63-67. doi:10.1016/S0022-0248(00)00060-9

[6] S. Yamauchi, Y. Goto and T. Hariu, "Photoluminescence Studies of Undoped and Nitrogen-Doped ZnO Layers Grown by Plasma-Assisted Epitaxt," *Journal of Crystal Growth*, Vol. 260, No. 1-2, 2004, pp.1-6. doi:10.1016/j.jcrysgro.2003.08.002

[7] D. C. Look, D. C. Reynolds, C. W. Litton, R. L. Jones, D. B. Eason and G. Gantwell, "Characterization of Homoepitaxial p-Type ZnO Grown by Molecular Beam Epitaxy," *Applied Physics Letters*, Vol. 81, No. 10, 2002, pp. 1830-1832. doi:10.1063/1.1504875

[8] B. K. Meyer, H. Alves, D. M. Hofmann, W. Kriegseis, D. Forster, F. Bertram, J. Christen, A. Hoffmann, M. Straßburg, M. Dworzak, U. Haboeck and A. V. Rodina, "Bound Exciton and Donor-Acceptor Pair Recombinations in ZnO," *Physica Status Solidi* (*B*), Vol. 241, No. 2, 2004, pp. 231-260.

[9] L. S. Vlasenko and G. D. Watkins, "Intrinsic Defects in ZnO: A Study Using Optical Detection of Electron Paramagnetic Resonance," *Physica B*, Vol. 376-377, 2006, pp. 677-681. doi:10.1016/j.physb.2005.12.170

[10] S. Yamauchi and Y. Imai, "ZnO Heteroepitaxy on Sapphire Using a Novel Buffer Layer of Titanium Oxide: Crystallographic Behavior," *Crystal Structure Theory and Applications*, Vol. 2, No. 2, 2013, pp. 39-45.

[11] S. S. Kurbanov and T. W. Kang, "Spectral Behavior of the Emission Around 3.31 eV (A-Line) from ZnO Nanocrystals," *Journal of Luminescence*, Vol. 130, No. 5, 2010, pp. 767-770. doi:10.1016/j.jlumin.2009.11.030

[12] A. Teke Ü. Özgür, S. Dogan, X. Gu, H. Morkoç, B. Nemeth, J. Nause, H. O. Everitt, "Excitonic fine Structure and Recombination Dynamics in Single-Crystalline ZnO," *Physical Review B*, Vol. 70, No. 19, 2004, Article ID. 195207-1-10.

[13] D. C. Reynolds, D. C. Look, B. Jogai, C. W. Litton, T. C. Collins, W. Harsch and G. Cantwell, "Neutral-Donor-Bound-Exciton Complexes in ZnO Crystals," *Physical Review B*, Vol. 57, 1998, pp. 12151-12155. doi:10.1103/PhysRevB.57.12151

[14] H. Alves, D. Pfisterer, A. Zeuner, T. Riemann, J. Christen, D. M. Hofmann and B. K. Meyer, "Optical Investigations on Excitons Bound to Impurities and Dislocations in ZnO," *Optical Materials*, Vol. 23, No. 1-2, 2003, pp. 33-37. doi:10.1016/S0925-3467(03)00055-7

[15] B. Gil, "Oscillator Strengths of A, B, and C Excitons in ZnO Films," *Physical Review B*, Vol. 64, 2001, Article ID. 201310-1-3. doi:10.1103/PhysRevB.64.201310

[16] B. K. Meyer, J. Sann, S. Lautenschläger, M. R. Wagner and A. Hoffmann, "Ionized and Neutral Donor-Bound Excitons in ZnO," *Physical Review B*, Vol. 76, 2007, Article ID. 184120-1-10. doi:10.1103/PhysRevB.76.184120

[17] H. Shibata, M. Watanabe, M. Sakai, K. Oka, P. Fons, K. Iwata, A. Yamada, K. Matsubara, K. Sakurai, H. Tampo, K. Nakahara and S. Niki, "Characterization of ZnO Crystals by Photoluminescence Spectroscopy," *Physica Status Solidi* (*C*), Vol. 1, No. 4, 2004, pp. 872-875.